

5-7-2008

## Channel Modeling for Vehicle-to-Vehicle Communications

David W. Matolak

University of South Carolina - Columbia, [matolak@cec.sc.edu](mailto:matolak@cec.sc.edu)

Follow this and additional works at: [https://scholarcommons.sc.edu/elct\\_facpub](https://scholarcommons.sc.edu/elct_facpub)



Part of the [Signal Processing Commons](#), and the [Systems and Communications Commons](#)

---

### Publication Info

Postprint version. Published in *IEEE Communications Magazine*, Volume 46, Issue 5, 2008, pages 76-83.

This Article is brought to you by the Electrical Engineering, Department of at Scholar Commons. It has been accepted for inclusion in Faculty Publications by an authorized administrator of Scholar Commons. For more information, please contact [digres@mailbox.sc.edu](mailto:digres@mailbox.sc.edu).

# Channel Modeling for Vehicle-to-Vehicle Communications

David W. Matolak, Ohio University

## ABSTRACT

Physical layer channel modeling is critical for design and performance evaluation at multiple layers of the communications protocol stack. In this article we describe and provide results for modeling vehicle-to-vehicle (V2V) wireless channels. V2V settings produce some unique conditions, and due to these conditions, V2V channels often exhibit greater dynamics than many conventional channels and, in addition, can also exhibit more severe fading. Thus, new channel models are needed to characterize this setting in order to evaluate contending transmission schemes and aid in V2V communication system design. A brief review of key statistical channel parameters is provided. Then both analytical and experimental V2V channel results are presented from the existing literature, and from our own measurement and modeling campaigns for the 5 GHz band. We also show the effects of these V2V channels on two types of transmission schemes.

## INTRODUCTION

Vehicle-to-vehicle (V2V) communication is expected to be an important facet of future intelligent transportation systems (ITSs) [1]. Hence, investigations on all aspects of ITS [2] are increasing. This includes studies at all levels of the communications protocol stack, as well as technology developments and field trials. Some obvious benefits of V2V communication are enhanced road safety; increased commuter awareness of current traffic [3], weather, and road conditions; reduced delays at tollbooths; and the ability to enable groups of traveling cars to exchange multimedia information. Vehicular mobile ad hoc networks (VANETs) are also receiving attention, and may be used by public safety organizations [4] and the military, as well as the general public. The list of possible applications is long, and is addressed by other articles in this issue.

Although a standard for V2V communication does exist (for the 5.9 GHz UNII band; the dedicated short-range communication, DSRC, standard) [1], this extension of the IEEE 802.11a wireless local area network (WLAN) standard may not suffice for all applications. As with most

WLAN standards, the standard in [1] specifies the transmission scheme at the lower two layers of the communications protocol stack. Yet as new V2V applications arise, newer standards to support these applications may be needed. Thus, newer schemes such as the IEEE 802.16e wireless metropolitan area (WMAN) standard may see application. The industry-developed set of technologies that will implement a subset of the large number of configurations of the 802.16e standard is often referred to as WiMAX. Some potential advantages of 802.16e over the modified 802.11a standard in V2V environments are its higher data rate, fast feedback channel for mitigating fading, and stronger forward error correction (FEC) coding for better performance. It is also possible that other standards may be applied in future V2V settings.

Regardless of the transmission technique employed, knowledge of the wireless channel is vital to the optimal design and performance of any V2V communication system [5]. It is well known that mathematical channel characterization results provide fundamental knowledge for all communication system physical layer waveform design and analysis. The use of thorough channel characterization information allows prediction and trade-off studies that affect various aspects of communication system design, such as optimal channel bandwidths and system performance (bit error ratio, latency, etc.) for *any* potential waveform used across the channel. Remedial measures (e.g., equalization, diversity) must also be designed based on channel knowledge. Thus, a primary use of channel models is in the evaluation and comparison of different transmission schemes<sup>1</sup> that can be deployed in the environment in question. In particular, these channel models are used as elements, or blocks, in a cascade of models that includes the other components in a wireless communication system. Although modern channel models contain mathematical descriptions that can be used for analysis, often analysis becomes intractable, at which point evaluation and trade-off can be conducted and extended via companion computer simulations. This is also a natural way to use models that are wholly empirical: those that “replay” measured channel data.

Even with a highly adaptive and reconfigurable communication system, if not taken into

<sup>1</sup> We use the term transmission scheme here to collectively represent both transmission and reception schemes.

account, the impairments caused by the channel may be severe enough to degrade performance significantly. Example outcomes of inadequately accounting for channel characteristics include a bit error probability (or bit error ratio, BER) “floor,” in which error probability reaches a lower limit regardless of received power level, and a large latency, which in the case of some protocols would translate to a link outage. The large latency could be caused, for example, by severe channel fading, which causes packet errors and forces the system to employ retransmissions. Retransmissions also reduce the achievable throughput, and this can significantly degrade both objective and subjective performance for many applications. Hence, channel characteristics also affect protocol design. Clearly the undesirable outcomes noted here should occur with very low probability, particularly for V2V applications related to safety.

There are well-known ways to mitigate such detrimental channel effects, some of which are prudently incorporated into the above mentioned transmission schemes. Mitigation techniques at the physical layer (PHY) include antenna diversity, strong FEC coding and interleaving, rapid power control, and equalization. At higher layers one may incorporate network coding and cooperative transmissions. Nevertheless, the efficient and effective design of these channel impairment mitigation techniques relies on good models for the wireless channel over which transmission takes place. This is the primary focus of this article.

We describe existing models for the V2V channel. We first briefly describe some of the main channel parameters needed to characterize a wireless channel, review both analytical and empirical models, and highlight key differences between V2V and more conventional channels. We also describe some existing models for the V2V channel. We provide some example results from measurements and corresponding models, highlighting new and unique V2V channel phenomena. We then summarize the article.

## V2V CHANNEL MODELS

### CHANNEL PARAMETERS

The study and modeling of wireless channels has many decades of history behind it, and for reasons of brevity we can provide only a cursory overview here. The V2V channel, in which both transmitter and receiver can be mobile, is a relatively newer area of study. Wireless channels can be modeled either deterministically, or statistically [5, 6]. For most applications, deterministic modeling is site-specific and computationally intensive; hence, statistical models are often more attractive in that they do not attempt to provide exact estimation of a channel’s small scale fading characteristics at points in space at any particular time; rather, they attempt to faithfully *emulate* the variation in these channel effects. Henceforth we focus primarily on statistical models. We also concern ourselves only with small scale fading, which most often arises due to the destructive interference from multiple replicas of the transmitted signal arriving at the receiver with different delays. This results from

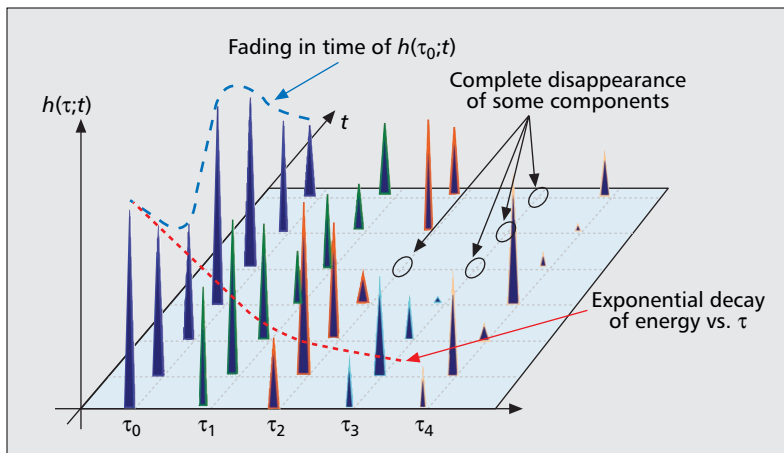
multipath propagation, and such fading is observed on spatial scales on the order of one-half wavelength. In contrast, for frequency bands of current interest (VHF and higher), large-scale fading (often termed shadowing, obstruction, or blockage) occurs on scales of many (e.g., 20 or more [5]) wavelengths. We first provide a very brief review of some important parameters used to characterize wireless channels. (See [5, 6] for a much more comprehensive review.)

The term *channel characterization* is used to describe the models, theory, and experimental data that constitute one’s knowledge of a wireless channel in a specific type of environment, typically a function of channel bandwidth and center frequency. One can define the channel as the complete set of parameters for all paths that transmitted electromagnetic waves in the frequency band of interest take from transmitter to receiver over the spatial region of interest. For engineering purposes, the characterization must be quantitative and as thorough as possible. Conversely, the thorough quantitative description must not be so complex as to limit its usefulness; thus, a balance is sought. The final characterization must also be in a form convenient for use in analysis, computer simulations, and experiment if it is to be widely employed. Most often, a mathematical (statistical) model for the time-varying channel impulse response (CIR) and its components constitutes the most useful characterization.

Broadly speaking, wireless channels can be either dispersive or nondispersive. A dispersive channel is strictly defined as one in which phase velocity is a function of frequency; hence, wideband signals are more likely to encounter dispersion than narrowband signals. This dispersion can also yield time spreading, or time dispersion of a signal. In the multipath propagation case, the effect of time dispersion arises from the different path lengths the multiple replicas of the transmitted signal travel. This could include a direct or line-of-sight (LOS) path, but also often includes multiple reflected paths. The multipath channel is said to be time-dispersive when the *spread* of these multiple received replicas in delay is on the order of a digital symbol duration ( $T_s$ ) or longer. The spread of the replicas is termed the delay spread, and in a statistical characterization, the root mean square (RMS) value is most often used. We use RMS-DS, or  $\sigma_\tau$ , to denote this measure of channel dispersion.

Since the wireless channel is well modeled as linear, we can characterize it completely in terms of its CIR or, equivalently, the Fourier transform of this, the channel transfer function (TF). The RMS-DS is the RMS value of the spread in delay of the power-weighted delayed multipath components when an impulse is input to the channel (strictly,  $\sigma_\tau$  is the RMS value of the autocorrelation of the CIR at any instant of time, but in practice, the CIR can only be sampled via measurements, and  $\sigma_\tau$  can be computed for each sample CIR or power delay profile, PDP). The CIR is often given as a function of two variables,  $h(\tau, t)$ , where, roughly,  $\tau$  is short-term delay, and  $t$  is the independent variable that allows for time variation; more precisely,  $h(\tau, t)$  is the output of the channel at time  $t$  due

*Broadly speaking, wireless channels can be either dispersive or non-dispersive. A dispersive channel is strictly defined as one in which phase velocity is a function of frequency, hence wideband signals are more likely to encounter dispersion than narrowband signals.*



■ **Figure 1.** Conceptual illustration of time-varying CIR.

to an impulse input at time  $t - \tau$ . For causal channels we always have  $h(\tau, t) = 0$  for  $\tau < 0$ , so we often plot  $h(\tau, t)$  vs.  $\tau$  for various instants of time, yielding sets of CIR samples or, roughly equivalently, “PDP samples.” If the channel is time-invariant (TI),  $h(\tau, t)$  is  $h(\tau)$ , the usual IR for a linear TI (LTI) system. Real channels also have an IR whose duration is finite. Figure 1 shows a conceptual example of the time-varying CIR. The (time-varying) channel TF  $H(f, t)$  is the Fourier transform of  $h(\tau, t)$  with respect to  $\tau$ .

In mobile channels time variation is commonly present, and this variation is typically characterized by correlation functions that measure the rate of change of CIR (or PDP) components or transfer function frequency components with respect to time. The scattering function  $S(t, \nu)$  measures the average power output of the channel as a function of the time delay ( $\tau$ ) and the resulting Doppler frequency ( $\nu$ ) due to motion. The approximate width of the scattering function in the Doppler variable is called the Doppler spread  $f_D$ , and measures the amount the channel

spreads a transmitted tone in frequency; this is sometimes also called frequency dispersion.

Thus, for a first order characterization of the channel, it is sufficient to have  $\sigma_\tau$  or its approximate reciprocal, the coherence bandwidth  $B_c$  (see sidebar), and  $f_D$  or its approximate reciprocal, the coherence time  $t_c$  (see sidebar). The coherence bandwidth is a measure of frequency selectivity of the channel, and the coherence time is a measure of time selectivity of the channel; hence, both are important to consider when designing and evaluating any communication system to be used on the channel.

Finally, on these general channel characteristics, channels are often assumed to be wide-sense stationary (WSS) in time, which implies uncorrelated Doppler shifts at different frequencies within the channel band. Similarly, scattering that occurs at different delays is often assumed to be uncorrelated scattering (US), which implies that the channel’s frequency response is WSS. These conditions are commonly combined to yield widely used WSSUS channel models.

Existing V2V channel models are often based on models for similar settings, the most obvious of which is the cellular radio channel. Many models exist for the cellular channel, and some models are even incorporated into cellular radio standards. In many of these models the channel characteristics (e.g.,  $\sigma_\tau$ ,  $f_D$ ) have been determined empirically from comprehensive measurement campaigns. Analytical models are also used. For most cases, the tapped delay line (TDL) structure is used for the channel model. This is a linear, finite IR, filter model for the CIR, and for statistical modeling the filter coefficients, or tap weights, are random processes. Figure 2 illustrates the structure, with the  $k$ th input data symbol denoted  $d_k$ , channel output symbol  $y_k$ , and  $k$ th tap weight  $h_k(t) = \alpha_k(t)e^{j\phi_k(t)}$ . The blocks labeled  $\tau_k$  denote delays, and in digital systems these delays are typically equal to the symbol period. In general, the  $d$ s,  $h$ s, and  $y$ s are

### More on Statistical Channel Parameters

In this sidebar we provide some additional description on statistical channel parameters. This description is also necessarily brief and incomplete, and interested readers are encouraged to see [5, 6] for more comprehensive discussions.

**Time varying CIR:**  $h(\tau, t)$  = response of channel at time  $t$  due to an impulse input at time  $t - \tau$ . Typically estimated via measured power delay profiles (PDPs) and phase information of each resolved multipath component. The most common statistic of the PDP is the RMS delay spread,  $\sigma_\tau$ .

**Time varying TF:**  $H(f, t)$  = Fourier transform of  $h(\tau, t)$  with respect to  $\tau$ .

**Spaced-frequency, spaced time (SFST) correlation function:**  $R(t, f, \Delta t, \Delta f)$  = correlation of the time varying TF, at time lag  $\Delta t$ , frequency separation  $\Delta f$ . When scattering at different delays is uncorrelated, and time variation is wide-sense stationary, this reduces to  $R(\Delta t, \Delta f)$ . The width of  $R(\Delta t, \Delta f)$  is called the coherence, or correlation, bandwidth  $B_c$ , which is a measure of correlation between channel effects at two different frequencies. As a very rough “rule of thumb,” we have  $B_c \approx 1/\sigma_\tau$ . The width of  $R(\Delta t, 0)$  is the coherence time,  $t_c$ , which is a measure of the time rate of change of the channel.

**Scattering function SF:**  $S(t, f, \nu, \tau)$  = average power output of the channel as a function of the time delay  $\tau$  and the resulting Doppler frequency  $\nu$  due to motion, taken at time  $t$ , frequency  $f$ . In general, this is the double Fourier transform of  $R(t, f, \Delta t, \Delta f)$  = correlation of the time varying TF, at time lag  $\Delta t$ , frequency separation  $\Delta f$ . For uncorrelated scattering and wide-sense stationarity, the SF reduces to  $S(\nu, \tau)$ , double Fourier transform of  $R(\Delta t, \Delta f)$ . The approximate width of  $S(\nu, \tau)$  in  $\nu$  is the Doppler spread  $f_D$ . As a very rough “rule of thumb,” we have  $f_D \approx 1/t_c$ .

### ■ Sidebar

complex, to compactly represent in-phase and quadrature components of bandpass signals and systems. The blocks labeled  $z_k(t)$  are binary (0,1) switching processes we describe in more detail subsequently.

The most common statistical model for the random tap amplitudes ( $\alpha$ s) is the Rayleigh fading model. The Rayleigh model arises from the Central Limit Theorem, in which both the in-phase and quadrature components of each tap are modeled as Gaussian. This Gaussianity requires that the multiple *subcomponents* which sum to create each tap be approximately equal-energy and large in number, although good approximations are often obtained when the number of multipath components in each tap is as small as 6–10 [5]. These subcomponents that make up each tap are received with approximately the same delay and are said to be unresolvable by the receiver, which occurs when their separation in delay is much smaller than the reciprocal of the signal bandwidth. Other common statistical models for random tap amplitude distributions include the Ricean, Nakagami, log-normal, and Weibull distributions [5].

Thus, to completely specify the TDL model for the channel, we need the number of taps (obtainable from  $\sigma_\tau$ ), their rate of change in time (obtainable from  $f_D$ ), and a statistical model for the tap amplitudes. (Unless there is a dominant, often LOS component, the tap phases are typically modeled as uniformly distributed on  $[0, 2\pi)$ .) Finally, we also require the relative energy of each tap. Typically the longer the delay, the weaker the multipath component, so an exponentially decaying power vs. delay characteristic is often employed (Fig. 1).

Even within a specific application area, channel models are often subdivided into classes, where each class aims to represent a particular type of physical situation. For the cellular channel, the rural, suburban, and urban classes are commonly used. For indoor channels, office and factory classes may be used. Some models also explicitly identify the presence of an LOS component, and divide into LOS and non-LOS (NLOS) cases. Also worth noting is that the V2V channel is by nature different from cellular and many other radio channels. Specifically in the V2V case, transmitter (Tx) and receiver (Rx) and some significant reflectors/scatterers are all mobile, the (typically) omnidirectional antennas for both Tx and Rx are at relatively low heights, and because of physical environment dynamics, the channel may be statistically *nonstationary*, which means tap amplitude distributions change over time/space. Over moderate spatial scales, reflectors/scatterers may “appear and disappear,” and this phenomenon can be modeled as a random on/off process for the multipath components. In this case we can model the CIR as follows:

$$h(\tau; t) = \sum_{k=0}^{L-1} z_k(t) \alpha_k(t) \exp\{j[\omega_{D,k}(t)(t - \tau) - \omega_c \tau_k(t)]\} \delta[\tau - \tau_k(t)], \quad (1)$$

where at time  $t$ ,  $\alpha_k(t)$  represents the  $k$ th resolved amplitude, and the argument of the exponential term is the  $k$ th resolved phase. The  $k$ th multipath component has a time-varying delay  $\tau_k(t)$ ,

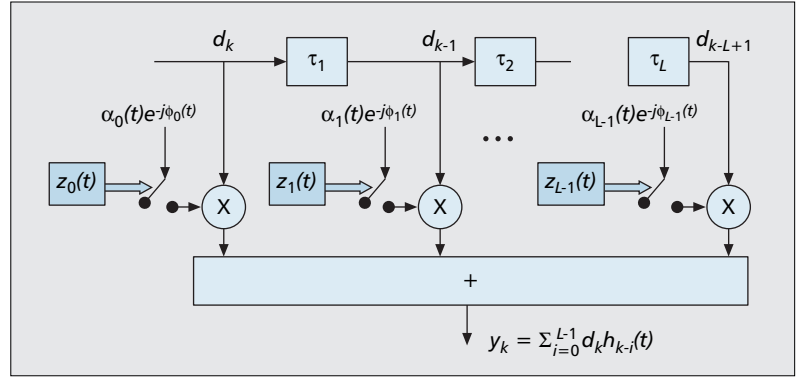


**Figure 2.** Tapped delay line model for a wireless channel, showing explicit multipath persistence (on/off) processes  $z_k(t)$ . Notation  $h_k(t) = \alpha_k(t) \exp[-j\phi_k(t)] z_k(t)$ ;  $k$ th switch is closed for  $z_k = 1$ , open for  $z_k = 0$ .

the  $\delta$ -function is a Dirac delta, the radian carrier frequency is  $\omega_c = 2\pi f_c$ , and the term  $\omega_{D,k}(t) = 2\pi f_{D,k}(t)$  represents the Doppler shift associated with the  $k$ th resolved multipath component, where  $f_{D,k}(t) = v(t) f_c \cos[\theta_k(t)]/c$ , where  $v(t)$  is relative velocity (also affected by scatterer velocity),  $\theta_k(t)$  is the aggregate phase angle of all components arriving in the  $k$ th delay bin, and  $c$  is the speed of light. The  $k$ th resolved component consists of multiple terms (subcomponents) from potentially different spatial angles  $\theta_{k,i}$  received in the  $k$ th delay bin. Compared to conventional representations of the CIR, we have an additional term in Eq. 1: the “persistence process”  $z_k(t)$ , used to account for the finite lifetime of the  $k$ th propagation path. As noted previously, V2V environments can induce frequent and rapid CIR changes due to mobility, and low transmitting and receiving antenna heights. The inclusion of this persistence process accounts for some of the “medium scale” channel variability in time, with multipath fading being small scale (i.e., distances of  $\sim 1/2$ ) and shadowing large scale (i.e., distances of many  $\lambda$ ).

### EXISTING V2V CHANNEL MODELS

For V2V channels, we briefly survey the literature and cite some examples of work; our survey is necessarily brief, and we invite the interested reader to consult the many references within each of our citations. One of the first references on the V2V channel was [7], in which the authors assume that small-scale fading has Rayleigh statistics. These authors generalized the work of Jakes [5], and derived new envelope autocorrelation functions and Doppler spectra. As expected, in the case when both transmitter and receiver are mobile, channel time variation can be more rapid than in the case when one or the other is motionless. The authors of [8] describe an effective means of simulating such a channel, using the sum of sinusoids (SoS) approach. Typically assumed in these models is isotropic scattering about both vehicles, applicable mostly in urban environments. These models also use the WSSUS assumption. In many V2V scenarios, isotropic scattering will be rare, and WSS conditions will pertain for a generally shorter time period than in single-mobile-platform cases. We illustrate this in the next section.

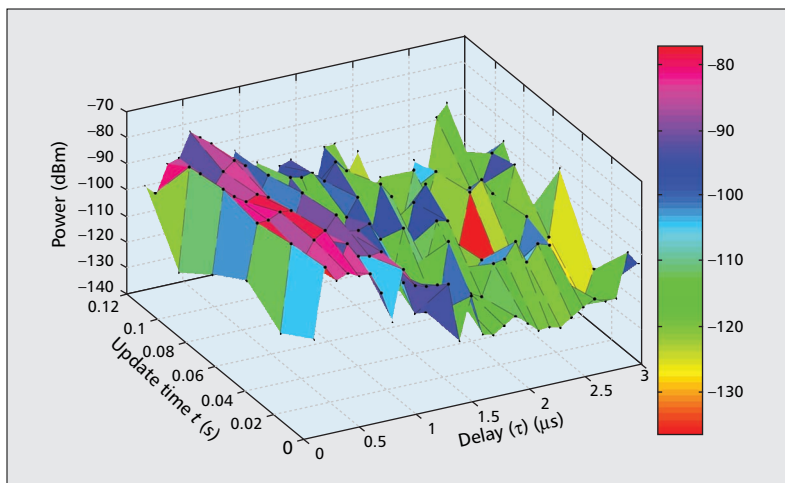


In [9] the authors studied the V2V channel for millimeter wave applications. Due to the large propagation path loss at millimeter wave frequencies, the authors assumed the use of directional antennas. An obvious limitation in using directional antennas is the difficulty of maintaining link connectivity between vehicles, except perhaps in some highway situations. In addition, most new V2V applications are expected to be in lower frequency bands (e.g., 5 GHz [1]) or the public safety band at 700 MHz [4]. With directional antennas the channel can be well modeled as having one LOS path and one or more reflected paths, and amplitude fading can be modeled as having Ricean statistics.

The authors of [10] employ a ray-tracing approach, and model typical roadside structures and vehicles as scattering objects with definable parameters. These authors have also published subsequent papers that elaborate on their models and analyze transmission system performance over their V2V channels. Although reasonably accurate ray-tracing channel models can be obtained for site-specific cases and generalized by random generation of object properties, the ray-tracing approach is generally computationally intensive (as most deterministic models are), and sacrifices accuracy if computational complexity is reduced.



■ **Figure 3.** View of transmitter van from receiver van on I-71 outside Cleveland, moderate to heavy traffic.



■ **Figure 4.** Measured power delay profiles for UIC V2V channel.

Reference [11] provides channel models for a number of different V2V settings, including expressway, urban canyon, and suburban street. Models are also provided for the roadside-to-vehicle channel. The models were developed from measurements in the 5.9 GHz band, and are designed for use with the DSRC standard, with bandwidth 10 MHz. Tapped delay line models are provided for these settings, with tap amplitude statistics either Rayleigh or Ricean. As with other work by these authors, tap Doppler spectra are also provided, yielding complete channel models. Worth noting is that the authors describe time-varying Doppler spectra, corresponding to statistically *nonstationary* conditions.

Finally, in this short review of V2V channel modeling literature we cite some of our own recent work, also in the 5 GHz band [12–14]. From our data we developed models for several V2V settings: urban, with antennas outside the cars (UOC); urban, with antennas inside the cars (UIC); small cities (S); and open areas (highways) with either high or low traffic densities (OHT and OLT). These models were designed for multiple values of bandwidth, including 5 MHz, 10 MHz, and 20 MHz. Unique in all our CIR models, we explicitly model the on/off switching process of each multipath component,  $z_k(t)$  in Eq. 1 (Fig. 2), via a first-order Markov chain. We also model tap amplitude statistics using the Weibull distribution, and in some cases we found fading worse than the common Rayleigh model. The Rayleigh model is almost universally used as a worst case model. We term this “worse than Rayleigh” fading *severe fading*, and as noted in [13], such severe fading has been reported in multiple environments at multiple frequency bands, but has only recently gained much attention in the research community. Physical mechanisms used to explain this severe fading include multiple scattering, rapid transitions of multipath components (e.g., multipath persistence), and in some cases a generalized Ricean model that allows for two dominant components plus the diffuse (scattered) components, in contrast to the conventional single-dominant-component Ricean case. Our models incorporate both statistical nonstationarity and severe fading to model the V2V channel as realistically as possible.

## EXAMPLE V2V CHANNEL MODELING RESULTS

We show results from [12–15] to illustrate features of V2V channels previously described. Figure 3 shows a photograph of our transmitting van on interstate I-71, between Cleveland and Columbus, Ohio. This was taken from the receiving vehicle, roughly 30 m behind, and in the center lane. This photo was taken near the end of rush hour, with traffic density thinning from heavy to moderate as we drove out of Cleveland. Figure 4 shows a power delay profile for the UIC setting, taken in downtown Columbus. The resolution in delay is 100 ns, and the update time is 20 ms. Fades of more than 20 dB are evident on some of the multipath components. This

figure has connected the components via a surface plot, but is analogous to the CIR shown in Fig. 1.

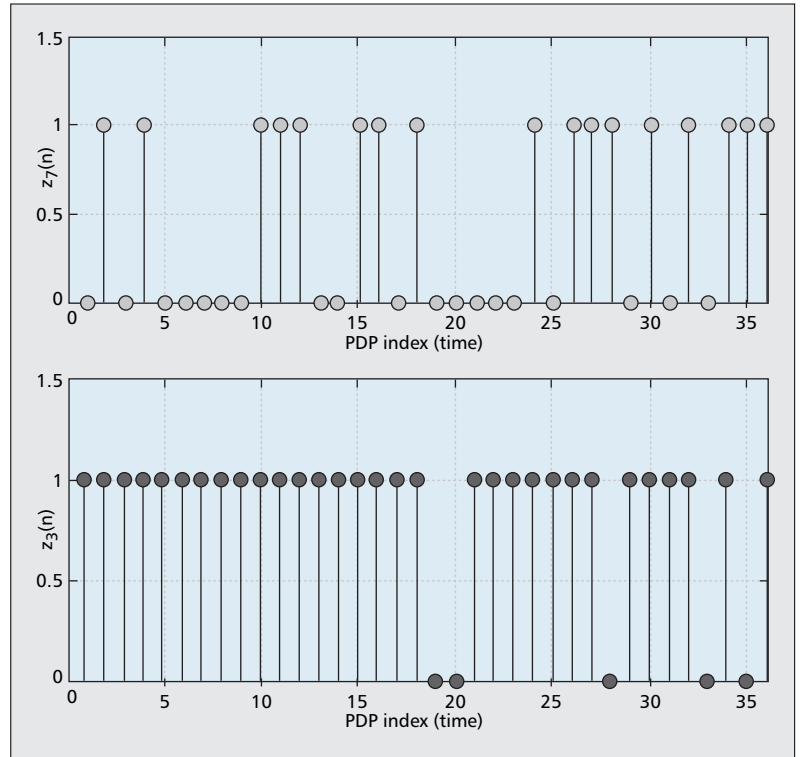
Figure 5 shows example tap persistence processes for some results obtained in a UOC setting. The figure shows the tap on/off behavior for tap 3 (bottom) and tap 7 (top). The plot in Fig. 5 can be viewed as tracing out the received power vs. a threshold for a fixed value of delay ( $\tau$  in Fig. 4). The threshold we used for declaring the presence/absence of a tap was 25 dB below the largest-amplitude component in a PDP. We chose this threshold value because larger values yielded essentially identical channel statistics. For the two taps shown in Fig. 5, tap 3 is above the threshold (and is hence on) for about 85 percent of the time, whereas tap 7 is above threshold (on) for only about 50 percent of the time. As noted, we model tap persistence with a first-order Markov chain, so each tap is described by its persistence parameters

$$TS = \begin{bmatrix} P_{00} & P_{01} \\ P_{10} & P_{11} \end{bmatrix}, \quad SS = \begin{bmatrix} P_0 \\ P_1 \end{bmatrix}, \quad (2)$$

where  $TS$  denotes transition probability matrix, and  $SS$  denotes the steady state probability vector. Element  $P_{ij}$  in matrix  $TS$  is the probability of going from state  $i$  to state  $j$ , and each  $SS$  element  $P_j$  gives the overall state occupancy probability for the  $j$ th state. For our multipath components, state 0 denotes off and state 1 denotes on. Typically longer delay taps (with larger tap index) have both smaller energy and smaller probabilities of being on (i.e., smaller  $P_1$  values) than shorter delay taps. Hence, in Fig. 5, tap 3 is on for a longer percentage of time than is tap 7. The Markov modeling parameters were extracted directly from all the PDP data of a given class. Note also that since the elements of Eq. 2 are probabilities, we have  $P_0 + P_1 = 1$ ,  $P_{00} + P_{01} = 1$ , and  $P_{10} + P_{11} = 1$ .

Table 1 provides channel parameters for constructing tapped delay line models for 10 MHz V2V channels, for three channel classes: UIC, S, and OHT [13]. The Weibull “shape” factor  $\beta$  is roughly analogous to the Ricean  $K$ -factor (which specifies the ratio of power in the LOS component to that in the diffuse components); the larger the value of  $\beta$ , the more benign the fading. A value of  $\beta = 2$  yields the Rayleigh distribution, and  $\beta$  values less than 2 are worse than Rayleigh, or severe fading. As Table 1 shows, severe fading occurs on a number of the channel taps, and the longer delay taps do not persist as long as the shorter delay taps.

We have also developed a simulation of the IEEE 802.16 standard and have run this simulation using our V2V channel models. Given the large number of configurations of the 802.16 transmission scheme, we show only representative results here for the orthogonal frequency-division multiple access (OFDMA) system similar to an uplink, in which multiple user signals are received by a reference user. We use a 10 MHz channel bandwidth, with 512 subcarriers, 408 of which are used for data transmission after removal of the dc and guard subcarriers. The OFDMA basic symbol time is 51.2  $\mu$ s, and the cyclic prefix length is 1.8  $\mu$ s, for a total sym-



■ **Figure 5.** Measured tap persistence processes for tap 3 (bottom) and tap 7 (top) for UOC V2V channel.

TAP index $K$	Energy	Weibull shape factor ( $\beta_K$ )	$P_{00,K}$	$P_{11,K}$	$P_1$
UIC					
1	0.756	2.49	NA	1.0000	1
2	0.120	1.75	0.0769	0.9640	0.9625
3	0.051	1.68	0.3103	0.8993	0.8732
4	0.034	1.72	0.3280	0.8521	0.8199
5	0.019	1.65	0.5217	0.7963	0.7017
6	0.012	1.6	0.6429	0.7393	0.5764
7	0.006	1.69	0.6734	0.6686	0.4971
Small city					
1	0.90	3.95	NA	1.0000	1.0000
2	0.08	2.0	0.4839	0.9446	0.9034
3	0.02	2.0	0.3452	0.7712	0.7383
OHT					
1	0.95	4.3	NA	1.0000	1.0000
2	0.04	1.64	0.3625	0.8366	0.7960
3	0.01	2.0	0.5999	0.6973	0.5696

■ **Table 1.** Channel models for 10 MHz UIC, S, and OHT channels.

bol time of 52.8  $\mu$ s. Modulation is 16-QAM, and we use the mandatory rate-1/2 convolutional code. We have five users transmitting, and consider the OHT and UOC channels, with Doppler spreads  $f_D = 458$  Hz for the OHT channel, and 286 Hz for the UOC channel. Figure 6 illustrates the BER performance for different simulation runs on these channels, with two values of  $E_b/N_0$ . The number of transmitted bits in each run is  $N_b = 14.2$  million, much larger than the value needed to obtain accurate results for a statistically stationary channel. Due to the channel nonsta-

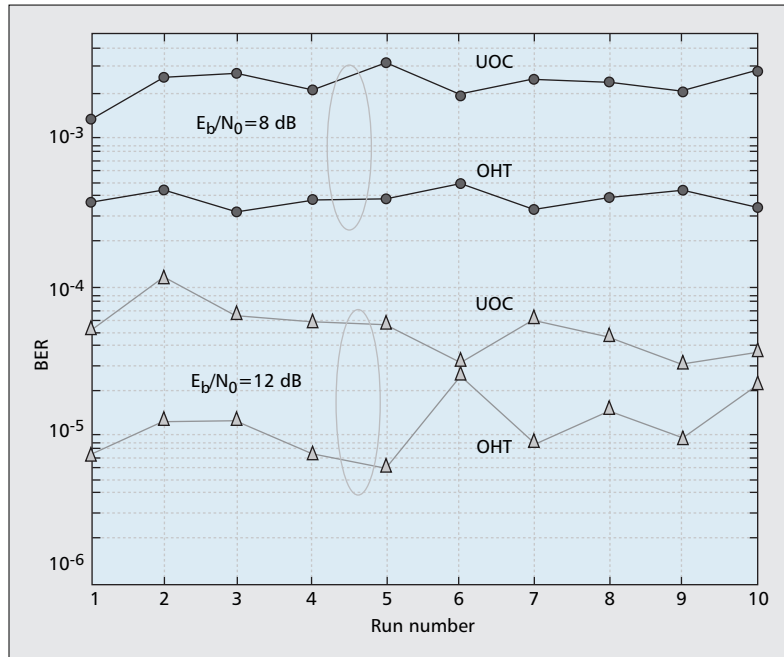


**Figure 6.** 802.16 BER vs. simulation run number for OHT and UOC V2V channels.

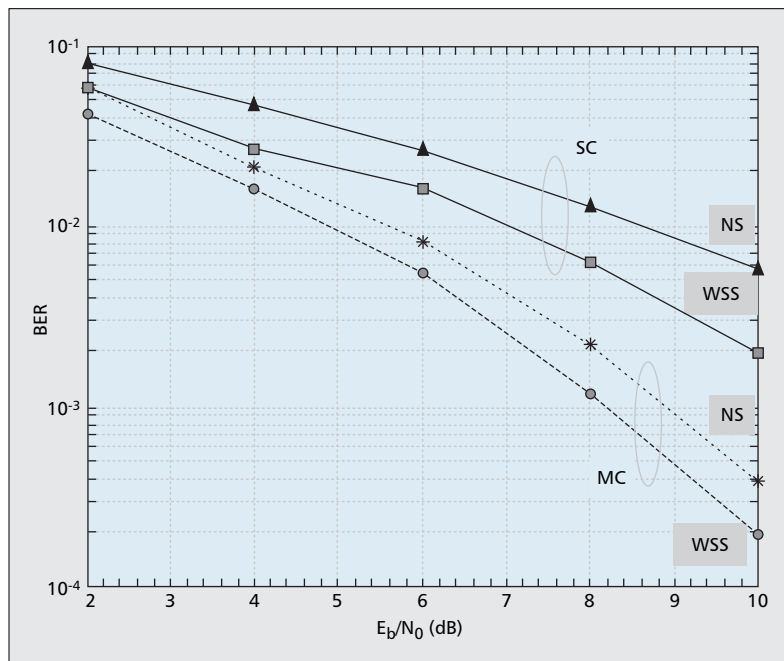


**Figure 7.** Single-carrier (SC) and multicarrier (MC, with three subcarriers) BER vs. SNR, UOC V2V channel. Both nonstationary (NS) and wide-sense stationary (WSS) channel model performance shown.

tionarity, we get different BERs for different runs, even though we are counting more than 500 errors in each run. BER variation of half an order of magnitude is apparent, and this variation is much larger for shorter runs with fewer packets, thus illustrating the importance of considering channel nonstationarity.

Finally, for two direct sequence spread spectrum (SS) systems, we show in Fig. 7 the BER vs. the bit-energy-to-noise-density ratio performance on the UOC 10 MHz V2V channel. Two SS systems were simulated, a single-carrier (SC) system with processing gain of 32, and a multicarrier (MC) system with three subcarriers and processing gain of 16. Total data rate and bandwidth of the systems is the same, and binary phase shift keying modulation is used with long random spreading codes. Single-user performance is shown for a wide-sense stationary version of the channel and our nonstationary version for both transmission schemes. Even though the MC system gains in performance over the SC system, both schemes suffer when the more realistic NS channel model is used, showing that the traditional WSSUS assumptions are optimistic and not necessarily valid for predicting performance in the V2V environment.

## SUMMARY

In this article we describe the importance of accurately modeling the V2V channel for future applications. After a review of important channel parameters, we show how the V2V channel differs from the channel in other settings, and can exhibit severe fading and statistical nonstationarity. Both these features should be taken into account when modeling the channel. We provide specifications for some 10 MHz V2V channel models we have developed from measurements, and show example performance results for IEEE 802.16 and spread spectrum transmission over these channels. These results illustrate the importance of using high fidelity channel models for predicting V2V system performance.

## ACKNOWLEDGMENTS

The author would like to thank his former doctoral students Indranil Sen, Wenhui Xiong, and Beibei Wang for their invaluable help in measurements, model development, and simulations prior to this work. Thanks also to the anonymous reviewers whose comments improved this article.

## REFERENCES

- [1] ASTM E2213, "Standard Specification for Telecommunications and Information Exchange between Roadside and Vehicle Systems — 5GHz Band Dedicated Short Range Communications (DSRC) Medium Access Control (MAC) and Physical Layer (PHY) Specifications," <http://www.astm.org>, Nov. 2007.
- [2] ITS project, <http://www.its.dot.gov/index.htm>, Nov. 2007.
- [3] S. Dashtinezhad et al., "Traffic View: A Driver Assistant Device for Traffic Monitoring based on Car-to-Car Communication" *Proc. IEEE VTC-Spring*, Milan, Italy, May 17–19, 2004.
- [4] T. L. Doumi, "Spectrum Considerations for Public Safety in the United States," *IEEE Commun. Mag.*, vol. 44, no. 1, Jan. 2006, pp. 30–37.
- [5] J. D. Parsons, *The Mobile Radio Propagation Channel*, 2nd ed., Wiley, 2000.



- 
- [6] P. Bello, "Characterization of Random Time-Variant Linear Channels," *IEEE Trans. Commun.*, vol. 11, Dec. 1963, pp. 360–93.
  - [7] A. S. Akki and F. Haber, "A Statistical Model of Mobile-to-Mobile Land Communication Channel," *IEEE Trans. Vehic. Tech.*, vol. VT-35, no. 1, Feb. 1986, pp. 2–7.
  - [8] C. S. Patel, G. L. Stuber, and T. G. Pratt, "Simulation of Rayleigh Faded Mobile-to-Mobile Communication Channels," *IEEE Trans. Commun.*, vol. 53, no. 11, Nov. 2005, pp. 1876–84.
  - [9] T. Tank, J-P M. G. Linnartz, "Vehicle to Vehicle Communications for AVCS Platooning," *IEEE Trans. Vehic. Tech.*, vol. 46, no. 2, May 1997, pp. 528–36.
  - [10] J. Maurer, T. Schafer, and W. Wiesbeck, "A Realistic Description of the Environment for Inter-Vehicle Wave Propagation Modelling," *Proc. IEEE VTC*, vol. 1, Oct. 2001, pp. 1437–41.
  - [11] G. Acosta-Marum and M. A. Ingram, "Six Time-and Frequency-Selective Empirical Channel Models for Vehicular Wireless LANS," *Proc. 1st IEEE Int'l. Symp. Wireless Vehicular Commun.*, Baltimore, MD, Sept. 30–Oct. 1, 2007.
  - [12] D. W. Matolak, I. Sen, and W. Xiong, "Channel Modeling for V2V Communications," (invited paper) *Proc. 2nd Int'l. Wksp. Vehicle-to-Vehicle Communications 2006*, San Jose, CA, 21 July 2006.
  - [13] I. Sen and D. W. Matolak, "Vehicle-Vehicle Channel Models for the 5 GHz Band," to appear. *IEEE Trans. Intelligent Transportation Sys.*
  - [14] B. Wang, I. Sen, and D. W. Matolak, "Performance Evaluation of 802.16e in Vehicle to Vehicle Channels," *Proc. IEEE VTC-Fall*, Baltimore, MD, 1–3 Oct. 2007.
  - [15] I. Sen and D. W. Matolak, "V2V Channels and Performance of Multi-User Spread Spectrum Modulation," *Proc. IEEE 1st Int'l. Symp. Wireless Vehic. Commun.*, Baltimore, MD, 30 Sept.–1 Oct. 2007.

## BIOGRAPHY

DAVID W. MATOLAK [M'83, SM'00] (matolak@prime.cs.ohiou.edu) received a B.S. degree from Pennsylvania State in 1983, an M.S. degree from the University of Massachusetts in 1987, and a Ph.D. degree from the University of Virginia in 1995, all in electrical engineering. He has more than 20 years of experience in communication system research, development, design, and deployment, with private companies, government institutions, and academia, including AT&T Bell Labs, L3 Communication Systems, The MITRE Corp., and Lockheed Martin. He has dozens of publications and several patents, and has expertise in spread spectrum, equalization, wireless channel characterization, and their application in both civil and military communication systems, including terrestrial, aeronautical, and satellite. He joined Ohio University School of Electrical Engineering and Computer Science in 1999.